Thallium-201 Uptake in Lung Cancer

Bennett B. Chin, Bruce W. Zukerberg, Carlos Buchpiguel and Abass Alavi

Division of Nuclear Medicine, Department of Radiology, Hospital of the University of Pennsylvania, Philadelphia, Pennsylvania

Key Words: thallium-201; technetium-99m-MIBI; lung carcinoma

J Nucl Med 1995; 36:1514–1519

CASE PRESENTATION

A 56-yr-old woman presented with a 1-yr history of chronic, nonproductive cough without chest pain, fevers or shortness of breath. Her past medical history was remarkable for hypertension, a 40-pack-per year history of smoking and sarcoidosis confirmed by mediastinoscopy 10 yr earlier. She was treated with oral antibiotics and cough suppressants, which resulted in partial improvement. Five months later, she presented with a 1-wk history of mild hemoptysis, persistent cough and a 10-lb weight loss. A chest radiograph demonstrated a large cavitating mass in the right upper lobe measuring approximately 10 cm in diameter (Fig. 1).

She was treated with antibiotics for possible postobstructive pneumonia and a metastatic workup was initiated. Bronchoscopy revealed no visible endobronchial lesions, but washings were positive for squamous-cell carcinoma. Computed tomography of the head and abdomen and a total body bone scan were all within normal limits. Computed tomography of the chest demonstrated a 7-cm right upper lobe mass with possible pleural and chest wall invasion as well as a 1-cm pretracheal lymph node (Fig. 2). The patient refused intervention and was discharged on oral antibiotics.

She returned 2 wk later with increasing cough and hemoptysis, persistent fevers, night sweats and occasional chills. Physical examination was unremarkable except for coarse rhonchi in the right middle lung field. Despite treatment with intravenous antibiotics, the fevers continued and chest radiographs remained unchanged. The patient then agreed to surgical intervention.

Preoperative evaluation included an exercise stress thallium SPECT myocardial perfusion study. No myocardial perfusion abnormalities were observed, but focal increased thallium uptake was present in the right upper lobe (Fig. 3).

Subsequently, a right upper lobe resection was performed. The gross specimen revealed a large tumor with central necrosis and hemorrhage. Focally, it extended through the pleural surface and grossly appeared to surround the third rib. Fourteen lymph nodes were removed with 1 hilar node appearing grossly positive for the tumor and measuring 2.5 cm in diameter. Microscopic evaluation of the tumor revealed invasive, poorly differentiated, focally keratinizing squamous-cell carcinoma with marked eosinophilic reaction without acute inflammation, extending up to but not through the pleural surface (Fig. 4). No tumor cells were found in neither the resected ribs nor in the 14 lymph nodes, including the 2.5-cm hilar node, which grossly appeared positive. Scant areas of acute inflammation were found in the lung tissue adjacent to the tumor. The patient's postoperative course was unremarkable.

Received Aug. 12, 1994; revision accepted Feb. 14, 1995.

For correspondence or reprints contact: Bennett B. Chin, MD, Johns Hopkins Hospital, 600 N. Wolfe St., Department of Radiology–Nuclear Medicine, B1-119 Nelson Bldg., Baltimore, MD 21287.

DISCUSSION

Thallium-201 myocardial perfusion scintigraphy is the most commonly performed nuclear cardiology procedure. Its extraction, washout and redistribution in myocardial cells has been well described; however, uptake in various malignancies has not been well characterized.

Thallium-201 Uptake in Malignancies

Following the intravenous administration of ^{201}Tl, radiotracer uptake occurs over time in the heart, liver, thyroid, salivary glands, colon, stomach, testes, eyes, kidneys and choroid plexus of the lateral ventricles (*1,2*). Uniform uptake is noted in all muscle groups (*1*). Thallium-201 is a potassium analog with myocardial uptake proportional to blood flow and extraction primarily mediated through the Na^+/K^+ ATPase system (*3,4*). Ouabain, an inhibitor of the Na^+/K^+ sarcolemmal ATPase pump, inhibits ^{201}Tl uptake into myocardial cells (*4*). In tumor cells, the mechanisms of ^{201}Tl uptake are not clearly defined. Sehweil et al. (*5*) demonstrated that ^{201}Tl uptake is dependent on blood flow as well as on the Na^+/K^+ ATPase system in tumor cells. Other possible contributing factors include tumor viability and type (*6*), an ion cotransport system (*7*), calcium ion channel exchange (*7*), vascular immaturity with leakage (*8*) and increased cell membrane permeability (*9*). In a study of cell localization, Ando et al. (*10*) reported that the majority of ionic thallium localized in intracellular fluid with only a small fraction bound to protein within the mitochondria, nucleus and microsomes. Peak tumor uptake in lymphoma and breast and lung carcinomas occurs at approximately 8–20 min after injection (*5,11*).

Several studies have been performed to investigate the use of thallium imaging in the detection of malignancy. In a preliminary study by Tonami et al. (*12*), 23 (100%) malignant pulmonary lesions, including primary adenocarcinoma, squamous-, small- and giant-cell carcinomas, sarcoma and metatstatic adenocarcinoma of the colon, were identified by thallium imaging with SPECT. In a subse-

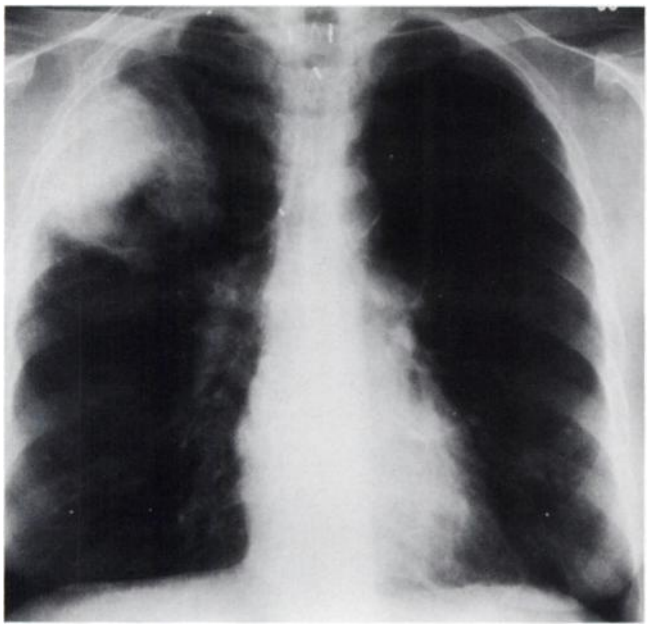

FIGURE 1. Chest radiograph visualizes a large cavitating mass in the right upper lobe.

quent report, Tonami et al. (*13*) reported visualization of 147 (100%) malignant pulmonary lesions in 170 patients with suspected malignant pulmonary lesions greater than 20 mm in diameter. These investigators did not include smaller lesions due to possible loss of sensitivity from partial volume effects. In addition, 16/23 (70%) benign lesions also had significant thallium uptake. An earlier investigation by Ochi et al. (*14*) reported a high specificity (90%) in differentiating benign from malignant thyroid tumors with delayed planar imaging. To classify focal thoracic uptake as malignant or benign, Tonami et al. proposed measuring a delayed ratio and a retention index from the early (15-min) and delayed (3-hr) postinjection SPECT images. The delayed ratio was defined as counts per voxel in the abnormal lung divided by counts per voxel in the contralateral normal lung. The retention index was defined as the difference between the delayed ratio and early ratio divided by the early ratio expressed as a percentage. No significant difference in the delayed ratio was seen when comparing benign to malignant lesions. A significant difference ($p < .01$) in the retention index, however, was noted between benign and malignant lesions. The retention indices for malignant and benign lesions were 25% ± 24% and 6% ± 14%, respectively (*13*). These authors concluded that the lack of thallium uptake in nodules larger than 20 mm effectively excluded malignancy, and that the use of the retention index was helpful in differentiating benign from malignant nodules.

Similarly, Suga et al. (*15*) evaluated 106 suspected malignant thoracic lesions greater than 20 mm in diameter with ^{201}Tl-SPECT imaging. All 48 (100%) malignant lesions and 39/58 (67%) benign lesions were visualized on the early scans. Benign conditions that showed early thallium uptake included active tuberculosis, active pneumonia, organizing pneumonia, inflammatory pseudotumor, silicosis, radiation pneumonitis, atypical mycobacterial disease, aspergilloma and granuloma. Suga's findings agreed with those of Tonami et al. (*13*) in that no significant difference was seen in the early or delayed uptake ratios in benign compared to malignant lesions. The difference in the retention index (−4.3% ± 13.6% for benign and 23.3% ± 18.9% for malignant lesions), however, was statistically significant ($p < .01$). For patients with a negative retention index or nonvisualization of ^{201}Tl uptake on delayed images, the classification of the lesion as benign had an accuracy of 81% and a predictive value of 95% (*15*).

Recently, Waxman et al. (*16*) reported excellent results with planar ^{201}Tl imaging in the detection of breast malignancy. In 81 women with palpable breast masses, ^{201}Tl detected 42/44 (96%) breast carcinomas. None of the 19 lesions with benign fibrocystic disease and neither of the 2 with fat necrosis showed ^{201}Tl uptake. Only three highly cellular adenomas of twenty-three adenomas were thallium avid, yielding a specificity of 91%.

Other investigators have reported similar results. Sehweil et al. (*17*) studied 188 patients with histologically confirmed carcinoma using planar ^{201}Tl imaging. Sensitivity of ^{201}Tl for detecting primary tumor (lung carcinoma 86%, breast carcinoma 100% and malignant lymphoma 85%) was high, but the detection rate was low (17%) for mediastinal or lymph node involvement. Similarly, Waxman et al. (*16*) reported a low 12/21 (57%) sensitivity in the detection of axillary node metastases from breast carcinoma. Sehweil et al. (*17*) reported increased ^{201}Tl uptake in benign conditions, including one case of active sarcoidosis and two cases of active tuberculosis, but delayed imaging was not performed.

Metastatic tumors to the thorax may also be visualized with thallium imaging. Increased uptake in metastatic thyroid carcinomas, parathyroid adenomas and lung and breast carcinomas have frequently been reported. Infrequently, cases of esophageal carcinoma, rhabdomyosarcoma, osteosarcoma, Ewing's sarcoma, germ cell tumor,

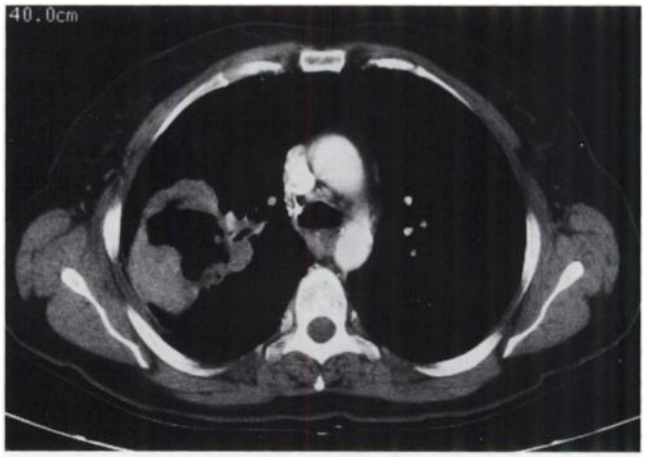

FIGURE 2. Chest CT shows large cavitating lesion in the right upper lobe, which appears to invade the thoracic wall.

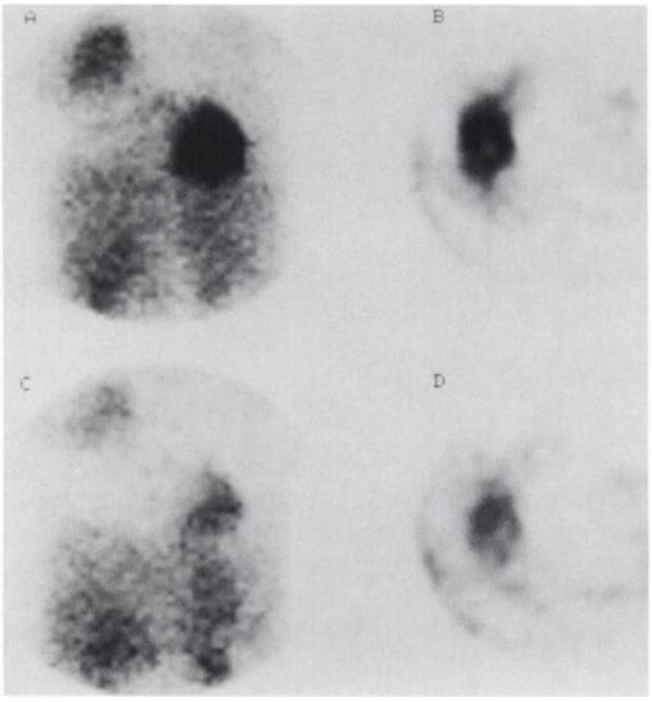

FIGURE 3. (A) Increased ^{201}Tl accumulation in the right upper lung is visualized on the anterior view from the exercise stress thallium SPECT projection images. (B) Transaxial reconstructed images (right chest is on left). Corresponding planar projection (C) and transaxial (D) images from the delayed study.

leiomyosarcoma, AIDS-related Kaposi's sarcoma (*1*), leukemic infiltration of the heart (*18*), rectal carcinoma, bladder carcinoma, gallbladder carcinoma and mesothelioma have also been reported to show thallium uptake (*15*). In patients with AIDS and pulmonary lesions, thallium imaging has been used with gallium imaging in the diagnosis of infectious and neoplastic processes. Both Kaposi's sarcoma and lymphoma incorporate ^{201}Tl in contrast to sites of infection, which are typically without thallium activity on delayed images. In the presence of thallium uptake, gallium may be used to distinguish lymphomas, which are gallium-avid, and Kaposi's sarcoma, which does not show gallium uptake (*19*).

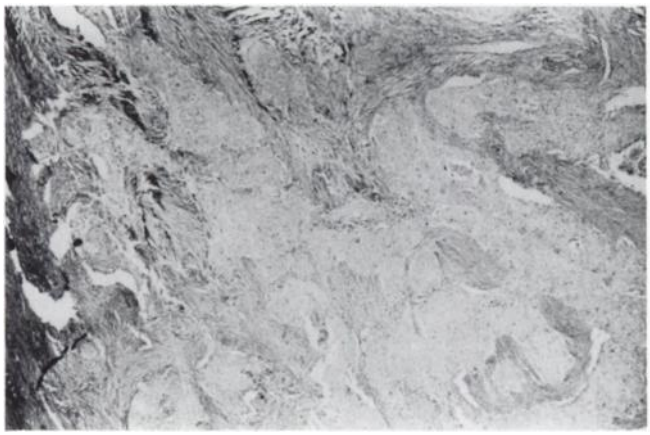

FIGURE 4. Histologic examination of the tumor reveals poorly differentiated, focally keratinizing squamous-cell carcinoma.

Without the use of delayed imaging or a retention index, cases of nonmalignant uptake of thallium in inflammatory and granulomatous disease processes have been reported. Active tuberculosis, silicosis, radiation pneumonitis, atypical mycobacterial pneumonitis, organizing pneumonia, inflammatory pseudotumor, aspergilloma, granulomas (*15*), highly cellular breast adenomas (*16*), sarcoidosis, abcess, sternotomy (*20*), atelectasis and cardioversion (*21*) have all been reported in association with extracardiac thoracic thallium uptake. Delayed imaging and retention indices in these nonmalignant conditions have not been studied in detail.

In addition to thoracic tumors, ^{201}Tl accumulates in a variety of other extrathoracic primary and metastatic tumors. Thallium-201 uptake in brain tumors, including malignant gliomas (*22*), astrocytomas and ependymomas (*23*), may be useful in distinguishing recurrent tumor from radiation necrosis. Imaging with ^{201}Tl is highly sensitive in detecting bone tumors, such as osteogenic sarcoma, and predicting therapeutic response (*1*). Without the use of delayed imaging, nonmalignant, early uptake of ^{201}Tl has also been reported in conditions of inflammation or increased blood flow, including trauma, fracture, Paget's disease, fibrous dysplasia, ossifying fibroma (*24*) and Brown tumors (*25*).

Technetium 99m-Sestamibi Uptake in Malignancies

Another single-photon tracer, ^{99m}Tc-hexakis-2-methoxyisobutyl isonitrile (MIBI) is currently being investigated for its potential in the detection of malignancies. Uptake of this tracer is normally present in the heart, thyroid and salivary glands, spleen, kidneys, bladder, lungs, skeletal muscle, liver, gallbladder and small and large intestines (*26,27*).

The mechanism of ^{99m}Tc-MIBI uptake in both myocardial and tumor cells has not been completely defined. Technetium-99m-MIBI is a lipophilic cation whose in vitro uptake and retention in various cell lines involves passive diffusion across plasma and mitochondrial membranes propelled by large negative transmembrane potentials (*28,29*). In vitro experiments have shown increased ^{99m}Tc-MIBI uptake with hyperpolarization and decreased uptake with depolarization of plasma and mitochondrial cell membrane potentials (*29*). Technetium-99m-MIBI uptake is less dependent than ^{201}Tl on active processes; uptake is unchanged by inhibitors of the respiratory chain, glycolysis or the Na^+/K^+ ATPase pump (*30*). In rat myocardial cells, almost 90% of MIBI is concentrated within the mitochondria as a free cationic complex (*31*). Irreversible binding to a cytosolic protein, previously thought to be the site of localization, was apparently an artifactual finding due to tissue homogenization and fractionation techniques (*31*). Cells with higher mitochondrial content, such as myocytes, concentrate more ^{99m}Tc-MIBI than quiescent cells such as those in the fibroblast family (*29,32*).

In vitro experiments with normal animal fibroblasts and nine selected human tumor cell lines (adenocarcinomas of the adrenal gland, lung, colon, and breast; undifferentiated pancreatic, poorly differentiated bladder, cervical and hepatocellular carcinomas; T-cell leukemia) have shown higher ^{99m}Tc-MIBI uptake in tumor cells compared to animal fibroblasts (*33*). A similar study with human breast and colon tumor cells showed higher ^{99m}Tc-MIBI uptake (5.37% ± 2.34%) compared to normal animal fibroblast cells (1.44% ± 1.88%) (*34*). These same cell lines were imaged with ^{201}Tl and showed higher uptake (5.39% ± 1.33%) in tumors compared to normal cells (3% ± 1.08%) (*34*).

Clinical experience with ^{99m}Tc-MIBI and thoracic malignancies is limited due to its relatively recent introduction. A preliminary study with ^{99m}Tc-MIBI reported localization in 10/11 untreated primary lung tumors, including adenocarcinoma, small-cell, squamous-cell and poorly differentiated germ-cell carcinomas (*35*). A subsequent study showed lower sensitivity with localization in 26/34 (76%) lung tumors (*36*). In a larger and more recent study, Kao et al. (*37*) evaluated 54 patients with a solitary lung mass and showed a sensitivity of 65%, specificity of 57% and an accuracy of 70% in differentiating benign and malignant lesions (*37*). Only 30/46 (65%) lung malignancies were detected by ^{99m}Tc-MIBI SPECT and 6/8 (75%) benign lesions were also visualized. Based on these results, it appears that ^{99m}Tc-MIBI is of limited utility in the investigation of solitary lung nodules (*37*). Unfortunately, these reports (*13,37*) did not specify which benign conditions were associated with ^{99m}Tc-MIBI uptake. Aktolun et al. (*35*) reported only two cases of diffuse ^{99m}Tc-MIBI uptake in nonmalignant fibrosing alveolitis. Preliminary results with ^{99m}Tc-MIBI in breast carcinoma have reported better results with a sensitivity of 96%, specificity of 87% and positive and negative predictive values of 82% and 97%, respectively (*38*).

Technetium-99m-MIBI uptake in non-Hodgkin's lymphoma and thyroid carcinoma have also been reported (*35,36*). Rare cases of thoracic uptake have been reported in pulmonary actinomycosis, giant lymph node hyperplasia, poorly differentiated germ-cell tumors, medullary thyroid carcinoma, malignant thymoma and metastatic undifferentiated mesenchymal lung tumors (*39*). As with ^{201}Tl, common extrathoracic malignancies reported with ^{99m}Tc-MIBI uptake include primary brain (*23*) and bone tumors (*40*).

Fluorine 18-Fluorodeoxyglucose Uptake in Lung Malignancies

Currently, there is no effective staging test for lung cancer and for the workup of solitary pulmonary nodules. The high spatial resolution of CT and MRI provide important information in determining the local extent of disease, relationship to airway and vascular structures and localization for diagnostic biopsy (*43*). These anatomic modalities, however, frequently cannot distinguish between benign and malignant etiologies. In a prospective staging study of bronchogenic carcinoma using CT, McLoud et al. (*44*) reported a sensitivity of 64% and a specificity of 62% when compared to mediastinoscopy and/or thoracotomy in 43 patients. Enlarged lymph nodes are frequently associated with nonmalignant disorders, including superimposed infection from centrally obstructing carcinomas. Conversely, mediastinal lymph nodes with metastases may appear within the normal limits in size. Clearly, lymph node size cannot predict the presence or absence of malignancy.

PET studies using [^{18}F]-fluorodeoxyglucose (FDG) have demonstrated excellent preliminary results in the investigation of malignant disorders. In a prospective evaluation of suspicious pulmonary nodules by plain radiographs, Kubota et al. (*45*) demonstrated a sensitivity of 83% and a specificity of 90% with FDG-PET imaging of tumor in 22 patients. Similarly, Gupta et al. (*46*) prospectively studied 20 patients with solitary pulmonary nodules. All 13 malignant solitary pulmonary nodules showed significant increased FDG uptake and 7 benign lesions showed no definite evidence of increased FDG uptake. In addition, differential uptake values clearly differentiated malignant from benign etiologies. Patz et al. (*47*) showed a sensitivity of 97% and a specificity of 100% for FDG-PET in distinguishing tumor recurrence from residual fibrosis in 38 patients treated for bronchogenic carcinoma. Whal et al. (*48*) identified 10 primary carcinoma sites and 15 metastatic foci with FDG-PET in 23 patients with breast cancer. Potential limitations include relatively low spatial resolution compared to CT or MRI and normal myocardial uptake which may obscure adjacent abnormalities. Although large studies that also include benign inflammatory and small malignant lesions are necessary to determine the role of PET imaging in the management of patients with cancer, these and other preliminary reports are quite encouraging.

Somatostatin Analog Uptake in Tumors

Recent developments in the synthesis of labeled thymidine compounds, amino acids and receptor binding drugs may also further enhance the role of this imaging technique in the evaluation of malignant disorders. Indium-111 and ^{123}I-labeled octreotide are somatostatin receptor analogs currently under investigation in a wide variety of tumors. Neuroendocrine tumors with high concentrations of somatostatin receptors, including meningiomas, pituitary tumors, insulinomas, gastrinomas, paragangliomas, medullary thyroid carcinomas, neuroblastomas, pheochromocytomas and carcinoids, have all shown good preliminary results (*49*). Breast and small-cell lung carcinomas with somatostatin receptors have also been successfully localized; however, these tumors may not always express somatostatin receptors. Compared to monoclonal antibodies, octreotide's smaller molecular weight allows more rapid clearance from the bloodstream, which results in better imaging characteristics. Preliminary studies have shown encouraging results in small-cell lung carcinomas with extensive disease (*50,51*). Octreotide uptake in lung tumors without somatostatin re-

ceptors and in other nonmalignant conditions, including granulomas and lymphomas, have also been reported (*49*). Reubi et al. (*52*) reported a high density of somatostatin receptors in the peritumoral veins, despite the absence of receptors in the tumor itself, suggesting an explanation for uptake in receptor negative tumors (*52*). Other potential radiotracers, including monoclonal antibodies to CEA and tumor cell surface receptors, have shown encouraging preliminary results and are currently under investigation (*48*).

CONCLUSION

As described above, preliminary studies with ^{201}Tl imaging and ^{99m}Tc-sestamibi have shown a high sensitivity in detecting lung and breast malignancies. Recent studies with delayed imaging have reported acceptable specificity compared to earlier reports. Further prospective studies are necessary to determine the role of various imaging modalities, including PET and single gamma emitters such as ^{201}Tl, ^{99m}Tc-sestamibi and radiolabeled somatostatin receptor agents in the management of patients with various malignancies.

REFERENCES

1. Nadel HR. Thallium-201 for oncological imaging in children. *Semin Nucl Med* 1993;23:243–254.
2. Atkins HL, Budinger TF, Lebowitz E, et al. Thallium-201 for medical use. Part 3: human distribution and physical imaging properties. *J Nucl Med* 1977;18:133–140.
3. Gehring PJ, Hammond PB. The interrelationship between thallium and potassium in animals. *J Pharmacol Exp Ther* 1967;155:187–201.
4. McCall D, Zimmer LJ, Katz AM. Kinetics of thallium exchange in cultured rat myocardial cells. *Circ Res* 1985;56:370–376.
5. Sehweil AM, McKillop JH, Milroy R, et al. Mechanism of ^{201}Tl uptake in tumours. *Eur J Nucl Med* 1989;15:376–379.
6. Waxman AD, Ramanna L, Said J. Thallium scintigraphy in lymphoma: relationship to gallium-67 [Abstract]. *J Nucl Med* 1989;30(suppl):915.
7. Sessler MJ, Geck P, Maul FD, et al. New aspects of cellular thallium uptake: Tl^+-Na^+-^{2}Cl-cotransport is the central mechanism of ion uptake. *Nucl Med* 1986;23:24–27.
8. Winchell HS. Mechanisms for localization of radiopharmaceuticals in neoplasms. *Semin Nucl Med* 1976;6:371–378.
9. Brismar T, Collins VP, Kesselberg M. Thallium-201 uptake relates to membrane potential and potassium permeability in human glioma cells. *Brain Res* 1989;500:30–36.
10. Ando A, Ando I, Katayama M, et al. Biodistribution of ^{201}Tl in tumor-bearing animals and inflammatory lesion induced animals. *Eur J Nucl Med* 1987;12:567–572.
11. Sehweil A, McKillop LH, Ziada G, et al. The optimum time for tumour imaging with thallium-201. *Eur J Nucl Med* 1988;13:527–529.
12. Tonami N, Shuke N, Yokoyama K, et al. Thallium-201 single photon emission computed tomography in the evaluation of suspected lung cancer. *J Nucl Med* 1989;30:97–1004.
13. Tonami N, Yokoyama K, Shuke N, et al. Evaluation of suspected malignant pulmonary lesions with ^{201}Tl single-photon emission computed tomography. *Nucl Med Commun* 1993;14:602–610.
14. Ochi H, Hisashi H, Fukuda T, et al. Thallium-201-chloride thyroid scintigraphy to evaluate benign and/or malignant nodules. *Cancer* 1982;50:236–240.
15. Suga K, Kume N, Orihashi N, et al. Difference in 201Tl accumulation on single photon emission computed tomography in benign and malignant thoracic lesions. *Nucl Med Commun* 1993;14:1071–1078.
16. Waxman AD, Ramanna L, Memsic LD, et al. Thallium scintigraphy in the evaluation of mass abnormalities of the breast. *J Nucl Med* 1993;34:18–23.
17. Sehweil AM, McKillop JH, Milroy R, et al. ^{201}Tl scintigraphy in the staging of lung cancer, breast cancer and lymphoma. *Nucl Med Commun* 1990;11:263–269.
18. Civelek AC, Brinker JA, Camargo EE, et al. Rest thallium-201 myocardial perfusion imaging in a patient with leukemic infiltration of the heart. *Eur J Nucl Med* 1992;19:306–308.
19. Lee VW, Fuller JD, O'Brien MJ, et al. Pulmonary Kaposi sarcoma in patients with AIDS: scintigraphic diagnosis with sequential thallium and gallium scanning. *Radiology* 1991;180:409–412.
20. Krasnow AZ, Collier BD, Isitman AT, et al. The clinical significance of unusual sites of thallium-201 uptake. *Semin Nucl Med* 1988;18:350–358.
21. Minamiji K, Sunako M, Fujino M, Kurogane H, Yoshida Y. Increased ^{201}Tl uptake by the chest wall following cardioversion. *Eur J Nucl Med* 1988;13:548–549.
22. Kaplan WD, Takvorian T, Morris JH, et al. Thallium-201 brain tumor imaging: a comparative study with pathologic correlation. *J Nucl Med* 1987;28:47–52.
23. O'Tuama LA, Treves ST, Larar JN, et al. Thallium-201 versus technetium-99m-MIBI SPECT in evaluation of childhood brain tumors: a within-subject comparison. *J Nucl Med* 1993;34:1045–1051.
24. Ramanna L, Waxman AD, Rosen G. Evaluation of Tl-201 uptake patterns in bone lesions: differentiation of benign and malignant processes. [Abstract]. *J Nucl Med* 1992;33(suppl):869.
25. Yang CJ, Seabold JE, Gurll NJ. Brown tumor of bone: a potential source of false-positive thallium-201 localization. *J Nucl Med* 1989;30:1264–1267.
26. Savi A, Gerundini P, Zoli P, et al. Biodistribution of Tc-99m methoxyisobutyl-isonitrile (MIBI) in humans. *Eur J Nucl Med* 1989;15:597–600.
27. Wackers FJ-Th, Berman DS, Maddahi J, et al. Technetium-99m-hexakis-2-methoxyisobutyl isonitrile: human biodistribution, dosimetry, safety, and preliminary comparison to thallium-201 for myocardial perfusion imaging. *J Nucl Med* 1989;30:301–311.
28. Piwnica-Worms D, Kronauge JF, Chiu ML. Uptake and retention of hexakis (2-methoxyisobutylisonitrile) technetium (I) in cultured chick myocardial cells: mitochondrial and plasma membrane potential difference. *Circulation* 1990;82:1826–1838.
29. Chiu ML, Kronauge JF, Piwnica-Worms D. Effect of mitochondrial and plasma membrane potentials on accumulation of hexakis (2-methoxyisobutylisonitrile) technetium (I) in cultured mouse fibroblasts. *J Nucl Med* 1990;31:1646–1653.
30. Maublant JC, Gachon P, Moins N. Hexakis (2-methoxy isobutylisonitrile) technetium-99m and thallium-201 chloride: uptake and release in cultured myocardial cells. *J Nucl Med* 1988;29:48–54.
31. Carvalho PA, Chiu ML, Kronauge JF, et al. Subcellular distribution and analysis of technetium-99m-MIBI in isolated perfused rat hearts. *J Nucl Med* 1992;33:1516–1521.
32. Caldwell JH, Mertens H, Linssen MC, et al. Uptake kinetics of technetium-99m-methoxyisobutylisonitrile and thallium-201 in adult rat heart endothelial and fibroblast-like cells in comparison to myocytes. *J Nucl Med* 1992;33:102–107.
33. Delmon-Moingeon LI, Piwnica-Worms D, Van den Abbeeke, Holman BL, Jones AG. Uptake of the cation hexakis (2-methoxyisobutylisonitrile)-technetium-99m by human carcinoma cell lines in vitro. *Cancer Res* 1990;50:2198–2202.
34. Maublant JC, Zhang Z, Rapp M, et al. In vitro uptake of technetium-99m-teboroxime in carcinoma cell lines and normal cells: comparison with technetium-99m-sestamibi and thallium-201. *J Nucl Med* 1993;34:1949–1952.
35. Hassan IM, Sahweil A, Constantinides C, et al. Uptake and kinetics of Tc-99m hexakis 2-methoxy isobutyl isonitrile in benign and malignant lesions in the lungs. *Clin Nucl Med* 1989;14:333–340.
36. Aktolun C, Bayhan H, Kir M. Clinical experience with Tc-99m MIBI imaging in patients with malignant tumors: preliminary results and comparison with Tl-201. *Clin Nucl Med* 1992;17:171–176.
37. Kao CH, Wang SJ, Lin WY, Hsu CY, Liao SQ, Yeh SH. Differentiation of single solid lesions in the lungs by means of single-photon emission tomography with technetium-99m methoxyisobutylisonitrile. *Eur J Nucl Med* 1993;20:249–254.
38. Khalkhali I, Mena I, Diggles L. Review of imaging techniques for the diagnosis of breast cancer: a new role of prone scintimammography using technetium-99m sestamibi. *Eur J Nucl Med* 1994;21:357–362.
39. Sutter CW, Joshi MJ, Stadalnik RC. Noncardiac uptake of technetium-99m MIBI. *Semin Nucl Med* 1994;24:84–86.
40. Caner B, Kitapci M, Unlü M, et al. Technetium-99m-MIBI uptake in benign and malignant bone lesions: a comparative study with technetium-99m-MDP. *J Nucl Med* 1992;33:319–324.
41. O'Doherty MJ, Kettle AG, Wells P, et al. Parathyroid imaging with technetium-99m-sestamibi: preoperative localization and tissue uptake studies. *J Nucl Med* 1992;33:313–318.
42. Taillefer R, Boucher Y, Potvin C, Lambert R. Detection and localization of parathyroid adenomas in patients with hyperparathyroidism using a single

radionuclide imaging procedure with technetium-99m-sestamibi (double-phase study). *J Nucl Med* 1992;33:1801–1807.
43. Libshitz HI. Computed tomography in bronchogenic carcinoma. *Semin Roentgenol* 1990;25:64–72.
44. McLoud TC, Bourgouin PM, Greenberg RW, et al. Bronchogenic carcinoma: analysis of staging in the mediastinum with CT by correlative lymph node mapping and sampling. *Radiology* 1992;182:319–323.
45. Kubota K, Matsuzawa T, Fujiwara T, et al. Differential diagnosis of lung tumor with positron emission tomography: a prospective study. *J Nucl Med* 1990;31:1927–1932.
46. Gupta NC, Frank AR, Dewan NA, et al. Solitary pulmonary nodules: detection of malignancy with PET with 2-F-18-fluoro-2-deoxy-D-glucose. *Radiology* 1992;184:441–444.
47. Patz EF, Lowe VJ, Hoffman JM, et al. Persistent of recurrent bronchogenic carcinoma: detection with PET and 2-[F-18]-2-deoxy-D-glucose. *Radiology* 1994;191:379–382.
48. Wahl RL, Cody RL, Hutchins GD, et al. Primary and metastatic breast carcinoma: initial clinical evaluation with PET with the radiolabeled glucose analogue 2-[F-18]-fluoro-2-D-glucose. *Radiology* 1991;179:765–770.
49. Krenning E, Kwekkeboom D, Bakker W, et al. Somatostatin receptor scintigraphy with ^{111}In-DPTA and ^{123}I-Tyr-octreotide: the Rotterdam experience with more than 1000 patients. *Eur J Nucl Med* 1993;20:716–731.
50. Leitha T, Megahdadi S, Woltz M, et al. The role of iodine-123-Tyr-3-octreotide scintigraphy in the staging of small-cell lung cancer. *J Nucl Med* 1993;34:1397–1402.
51. Kwekkeboom D, Krenning EP, Bakker WH, et al. Radioiodinated somatostatin analog scintigraphy in small cell lung cancer. *J Nucl Med* 1991;32:1845–1848.
52. Reubi JC, Horisberger U, Laissue J. High density of somatostatin receptors in veins surrounding human cancer tissue: role in tumor-host interaction? *Int J Cancer* 1994;56:681–688.